

pubs.acs.org/macroletters Letter

Grafting-from Synthesis of Plant—Polynorbornene Biohybrid Materials

Luis Palomino, Ivonne Gonzalez-Gamboa, Moises Garcia-Mendoza, Andrea G. Monroy-Borrego, Lisa Tang, Bin Wang, Andrea Tao, Jinhye Bae, Nicole F. Steinmetz,* and Jonathan K. Pokorski*



Cite This: ACS Macro Lett. 2024, 13, 726–733



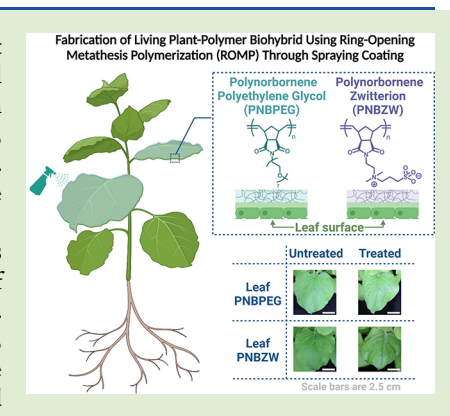
ACCESS I

III Metrics & More

Article Recommendations

Supporting Information

ABSTRACT: Plants, essential for food, oxygen, and economic stability, are under threat from human activities, biotic threats, and climate change, requiring rapid technological advancements for protection. Biohybrid systems, merging synthetic macromolecules with biological components, have provided improvement to biological systems in the past, namely, in the biomedical arena, motivating an opportunity to enhance plant well-being. Nevertheless, strategies for plant biohybrid systems remain limited. In this study, we present a method using grafting-from ring-opening metathesis polymerization (ROMP) under physiological conditions to integrate norbornene-derived polymers into live plants by spray coating. The approach involves creating biological macroinitiators on leaf surfaces, which enable subsequent polymerization of norbornene-derived monomers. Characterization techniques, including FTIR spectroscopy, SEM EDS imaging, ICP-MS, nanoindentation, and XPS, confirmed the presence and characterized the properties of the polymeric layers on leaves. The demonstrated modifiability and biocompatibility could offer the potential to maintain plant health in various applications, including the development of thermal barriers, biosensors, and crop protection layers.



Plants are essential for humanity, serving a vital role in nearly every aspect of modern society. They not only produce 80% of the food we consume and supply 98% of the oxygen we breathe, but also regulate the climate, generate valuable molecules, contribute to clean energy, and bolster the economy. This economic importance is particularly evident, as plants serve as the primary source of income for rural communities through agriculture. Consequently, the well-being of plants is critical for our ability to combat hunger, preserve the environment, develop sustainably derived alternatives for medicine, and promote economic development.²

Unfortunately, the health of plants is under increasing threat due to human activities, various biotic threats, and climate change. The combined impact of these factors is jeopardizing plant health through alterations in ecosystems, rising temperatures, shifts in precipitation patterns, sea-level rise, and the creation of more favorable conditions for pests and pathogens. For instance, in the agricultural arena, there has been a marked contraction in the rate of global agricultural productivity growth, attributed to the impact of abiotic and biotic stressors on plant well-being. Therefore, prompt technological developments are required to shield plants from these hazards, guaranteeing not only their survival but also the invaluable benefits they provide, such as maintaining clean air and ensuring food security.

Biohybrid systems that combine synthetic macromolecules with biological systems, such as proteins or cells, have helped to overcome limitations, mainly in the biomedical field.^{5–7}

Engineered for the realm of cell-based therapies, cell—polymer biohybrids have been designed to enhance cellular protection and imbue new functionalities to cells and tissues.^{8,9} Furthermore, biohybrids of proteins and polymers have demonstrated increased protein stability and a lowered potential for protein immunogenicity, making them advantageous for the development of protein therapeutics.^{7,10}

Despite these advancements, the exploration of polymer integration to more complex biological systems, such as living plants, remains largely unexplored. Limited research has focused on the integration of conductive polymers through the self-organization of these polymers within the inner structures of *ex vivo* plant matter or through *in vivo* polymerization within the root systems of intact plants. ^{11–13} Another innovative approach was developed to manipulate leaf morphology, which includes adhering 3D printable stimuliresponsive gels onto the surface of decellularized leaves. ¹⁴ An alternative striking example detailed flame retardant coatings using spray coating with viscoelastic fluids to large areas of vegetation. ¹⁵ While these strides represent significant progress

Received: May 7, 2024 Accepted: May 14, 2024 Published: May 29, 2024





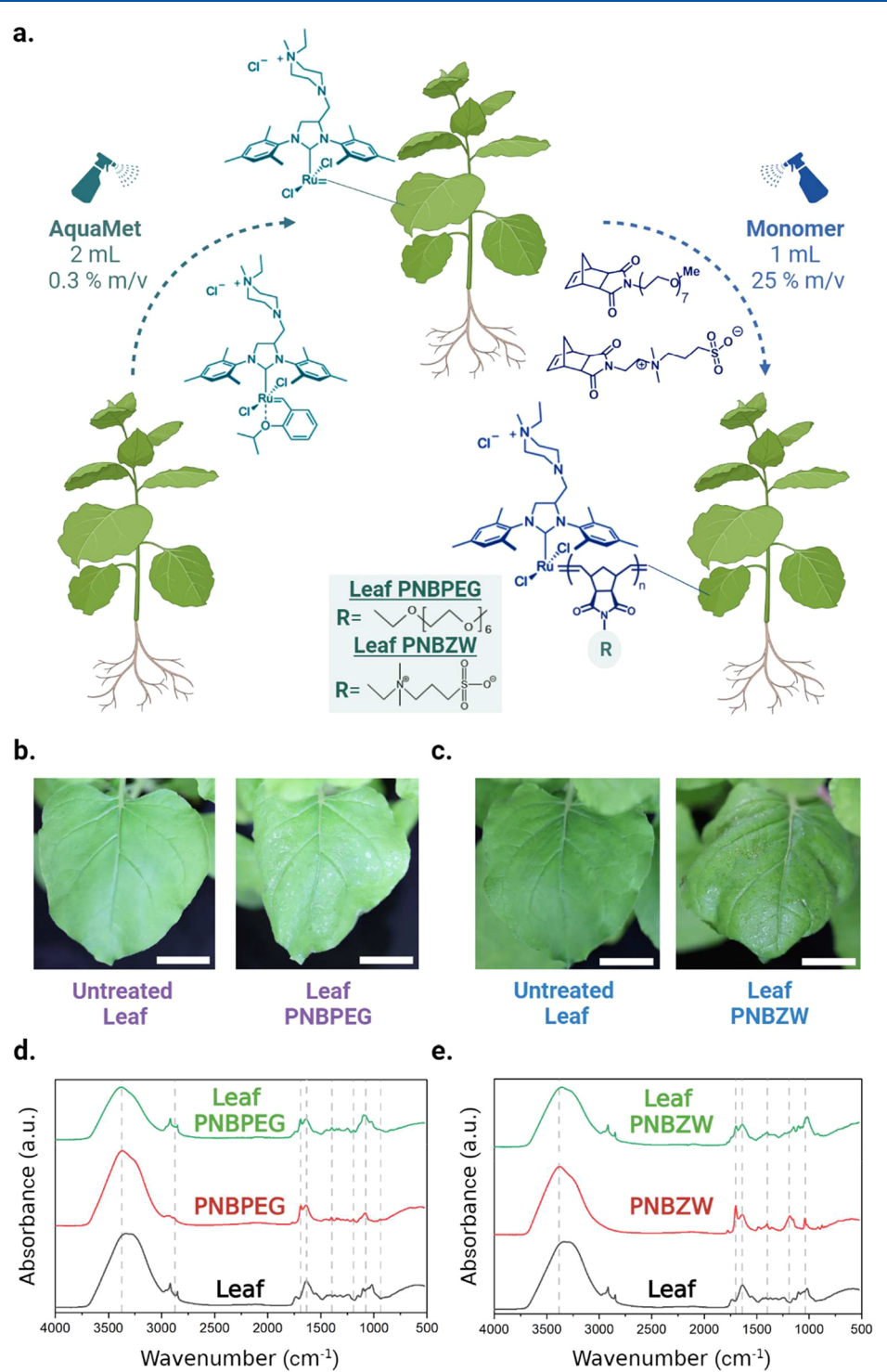


Figure 1. Living plant—polynorbornene derived polymer biohybrid systems. (a) Schematic representation of the spray-coating-based process. *Nicotiana benthamiana* leaves were modified with AM followed by NBPEG and NBZW for the formation of Leaf PNBPEG and Leaf PNBZW. Leaves before and after incorporation of (b) PNBPEG and (c) PNBZW. Scale bars are 2.5 cm. FTIR spectra of untreated and treated leaves for (d) Leaf PNBPEG and (e) Leaf PNBZW.

in the field of plant-polymer biohybrids, the strategies for fabrication still remain limited.

Ideal solutions are scalable strategies that would allow polymerization with modifiable architectures on the surface of living plants, enabling the installation of different functionalities to protect plants from external stressors. To address the scalability challenge, one proposed approach involves depositing polymer solutions using spray coating. ¹⁶ This method

allows for large-scale fabrication and can be implemented using unmanned aerial vehicles or robots. Additionally, achieving polymerization on plant surfaces would be accomplished through a biocompatible methodology, producing a versatile, comfortable, lightweight polymer to avoid a stress response from the plants, which are sensitive to mechanical stimulation.

We have recently pioneered the biocompatible synthesis of polynorbornene-derived polymers through ring-opening meta-

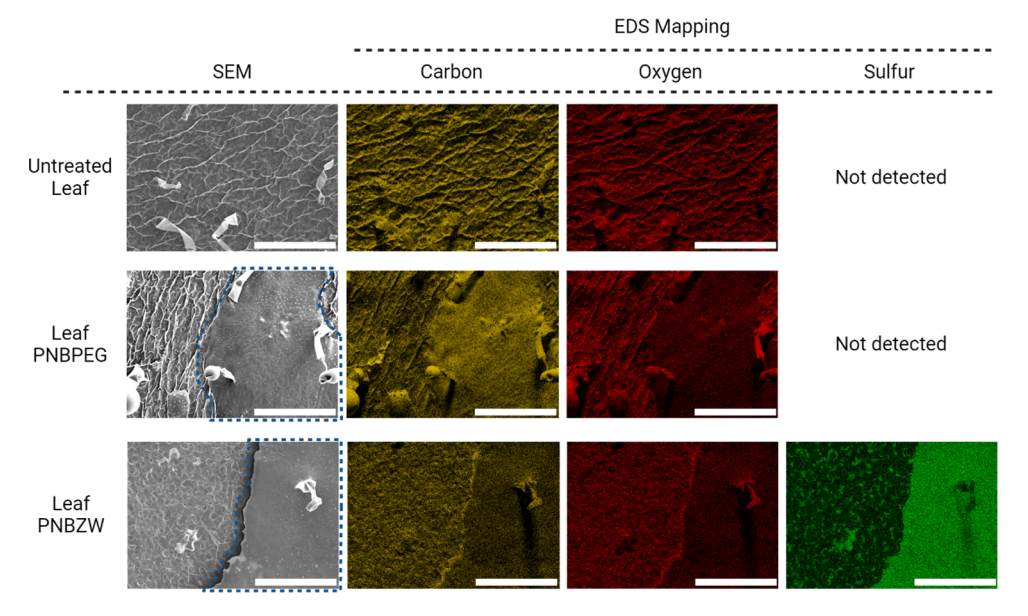


Figure 2. Scanning electron microscopy (SEM) images of untreated leaf and leaves after modification. In the first column, dashed lines demarcate areas of polymerization. Energy-dispersive spectroscopy (EDS) mapping demonstrates the presence of C and O corresponding to PNBPEG in Leaf PNBPEG. Similarly, the presence of C, O, and S from PNBZW is presented in Leaf PNBZW. Scale bars are 250 μ m.

thesis polymerization (ROMP) under physiological condi-This approach has facilitated the rapid integration of polymers with controlled molecular weight distribution and well-defined functional block copolymers at biological interfaces. 6,7,10,19-21 We envisioned that employing this strategy would enable us to introduce block copolymers onto the surface of leaves of living plants without compromising their survival and preserving their versatility for future modifications. Thus, in the future, we could envision complex polymers which could serve as antimicrobial or antifungal agents, superhydrophilic polymers for moisture retention, superhydrophobic polymers for excess water protection or polymeric layers which actively respond to external factors serving as biosensors. Herein, we describe a method to covalently tether highly functional polymers to the surface of leaves via a grafting-from ROMP spray coating approach.

To synthesize plant-polymer biohybrids, we chose the upper surface, adaxial side, of intact four week old Nicotiana benthamiana leaves to be modified by the polymerization of two types of monomers: norbornene polyethylene glycol imide (NBPEG), which leads to the formation of polynorbornene polyethylene glycol imide-modified leaves (Leaf PNBPEG), and norbornene zwitterionic sulfobetaine (NBZW), which is used for the formation of polynorbornene zwitterionic sulfobetaine-modified leaves (Leaf PNBZW; Figure 1a). To first create the biological macroinitiators on the surface of living plants, we focused on the outer layer of the leaves, known as the cuticle, as the modifiable unit. This layer primarily consists of very-long-chain fatty acids (VLCFAs) in the epicuticular wax (exterior layer) and hydroxy fatty acids (HFAs) in the proper cuticle (interior layer). 22,23 The presence of VLCFAs and HFAs on the surfaces of the leaves exposes double bonds for the functionalization of external molecules.² Given the capability of Ru-catalysts to react with long-chain olefins, 25-27 we spray-coated Aquamet (AM) onto the surface of the leaf with the intent to insert into the double bonds in the cuticle. AM is a commercially available Grubbs-Hoveyda catalyst, which we have previously optimized for polymerization under aqueous conditions. It is recognized that other

potential interactions may have occurred for surface anchoring, such as hydrophobic associations, however, it is nearly impossible to quantify on a heterogeneous leaf surface. Following macroinitiator formation, leaves were washed with water to remove any noncovalent or nonstrongly associated catalyst. The norbornene-derived monomer solutions were then sprayed onto the leaves, resulting in the formation of a transparent shiny polymeric layer on the treated areas. These polymeric layers were heterogeneously distributed across the leaf surface, leading to both covered and uncovered areas (Figure 1b, 1c).

The modified leaves exhibited surface-level structural alterations, which were attributed to the polymer growth from the leaf surfaces. Despite extensive efforts to mechanically detach or extract the polymer using solvents, these attempts were unsuccessful due to the polymer's strong adhesion to the leaf surfaces. Consequently, surface-initiated polymerizations were evaluated using surface characterization techniques such as Fourier transform infrared spectroscopy (FTIR), scanning electron microscopy (SEM), X-ray photoelectron spectroscopy (XPS), and nanoindentation, with FTIR initially used to study the surface alterations. In the biohybrid system Leaf PNBPEG, the main peaks of the PNBPEG polymer were identified, confirming their presence and their overlap with the peaks associated with the leaves (Figure 1d). Specifically, the appearance of O-H stretching and H-O-H bending at 3374 and 1634 cm⁻¹, respectively, is associated with the polymer absorbing moisture in the air. The stretching vibration of -C-H at 2874 cm⁻¹ originates from the PEG units from the polymer. Carbonyl stretching from the conjugated anhydride is observed at 1693 cm⁻¹. The bending motion of -C-H is noted at 1397 cm⁻¹, while the stretching peak of -C-N is observed at 1192 cm⁻¹. Finally, the -C-O stretching motion from the PEG structures is found at 1079 cm⁻¹, and the bending of the -C=C- that connects the monomers occurs at 938 cm⁻¹.

Similarly, the biohybrid system Leaf PNBZW showed characteristic peaks from the polymer in addition to the peaks from the leaves (Figure 1e). Peaks related to the polymer

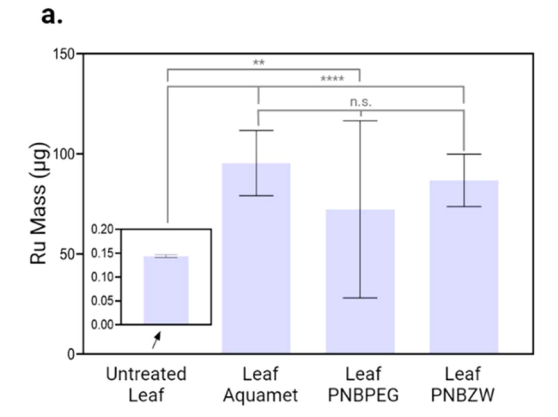
retention of moisture are found at 3384 and 1641 cm⁻¹. The C=O stretching from the anhydride ring is detected at 1670 cm⁻¹. At 1398 cm⁻¹, there is an observed bending motion of -C-H, and at 1191 cm⁻¹, a stretching peak related to -C-N is identified. The stretching of S=O bonds in the sulfoxide groups of the sulfobetaine units within the polymer is identified at 1038 cm⁻¹.

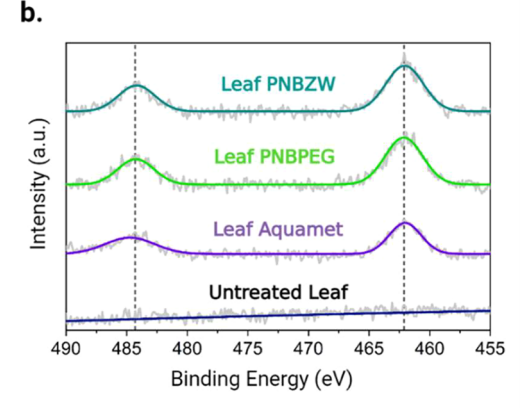
The morphological differences between untreated leaves and modified leaves were examined using SEM. Untreated leaves displayed a rough surface with hair-like outgrowths known as trichomes. In contrast, the polymeric areas in the modified leaves exhibited a smoother appearance (Figure 2). The distribution of these polymeric layers across the surface was somewhat heterogeneous. This lack of consistent coverage could influence the maintenance of essential physiological structures and their functionality either positively or negatively, depending on the desired application. Finally, in the case of Leaf PNBZW, we observed shadows resulting from differences in the topography, indicating a thicker polymeric layer compared to Leaf PNBPEG. Control samples, including leaves treated solely with AM (Leaf Aquamet), those treated solely with monomers, or those treated with monomers first followed by AM, were tested. The results clearly show the absence of polymer grafting or incorporation (Figure S1). The absence of polymer formation in controls where monomers were sprayed before the addition of AM may stem from hydrophilic monomers not uniformly coating the hydrophobic plant leaf surface. Additionally, the washing steps during the biohybrid system fabrication process likely removed any remaining monomer.

To further investigate the elemental composition of these polymeric layers on the leaves, energy-dispersive spectroscopy (EDS) mapping was performed. The elemental composition of the untreated leaves primarily consisted of carbon and oxygen. Similarly, in Leaf PNBPEG, the polymeric layer was predominantly composed of oxygen and carbon. In contrast, Leaf PNBZW showed the same composition in the PNBZW layer, but also displayed the presence of sulfur, attributable to the sulfonate group in the PNBZW structure.

The quantification of ruthenium originating from the AM catalyst was conducted using inductively coupled plasma mass spectrometry (ICP-MS). In untreated plants, the ruthenium content was measured at $0.14 \pm 0.001~\mu g$. Conversely, after the macroinitiators were formed in Leaf Aquamet, there was a significant increase in ruthenium levels, with a measurement of 95.41 \pm 16.33 μg . Similarly, the subsequent formation of the polymers on the leaves in Leaf PNBPEG and Leaf PNBZW, led to higher levels of ruthenium, with amounts of 72.27 \pm 44.25 μg and 86.76 \pm 13.07 μg , respectively (Figure 3a). In the leaf PNBZW case, the higher mean Ru concentration appears to correlate to a more complete coating, which aligns with the observation of a thicker polymeric layer in this sample compared to the polymeric layer in Leaf PNBPEG (Figure 2).

The oxidation state of ruthenium in the polymeric layers of the treated leaves (Figure 1a) was evaluated by XPS (Figure 3b). In the binding energy region of Ru 3p (490 eV - 455 eV), no peaks were observed in untreated leaves. In Leaf Aquamet two peaks were detected at 484.33 and 462.33 eV, corresponding to $3p_{1/2}$ and $3p_{3/2}$, respectively. These peaks were also observed in the polymerized leaves Leaf PNBPEG and Leaf PNBZW. These binding energies correspond to Ru^{2+} $\frac{28-30}{9}$ Because the oxidation state of Ru in the AM catalyst





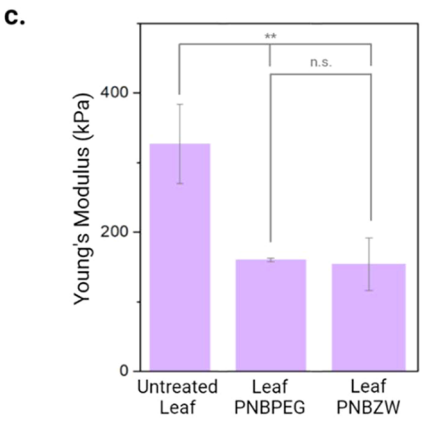


Figure 3. (a) Inductively coupled plasma mass spectrometry (ICP-MS) for the detection of Ru. Five measurements were taken from three distinct leaves per sample (b) X-ray photoelectron spectroscopy (XPS) in the Ru 3p region showing the presence of Ru⁺². (c) Nanoindentation showing a lower Young's modulus in modified leaves.

is considered +2, 31,32 this result validates the presence of ruthenium from AM in the modified leaves.

To analyze how the mechanical properties of the leaf are impacted by polymerization, the local Young's modulus of the leaf surface was measured using nanoindentation. In the absence of a polymer, the leaves presented a modulus of 326.7 \pm 57.2 kPa; however, when PNBPEG and PNBZW are polymerized directly on the surfaces of the leaves, the modulus decreased to 106.3 \pm 2.4 and 153.9 \pm 37.9 kPa, respectively (Figure 3c). This reduction in modulus is attributed to the polymers on the surface, since these polymers are viscous liquids when prepared neat. The presence of a softer material

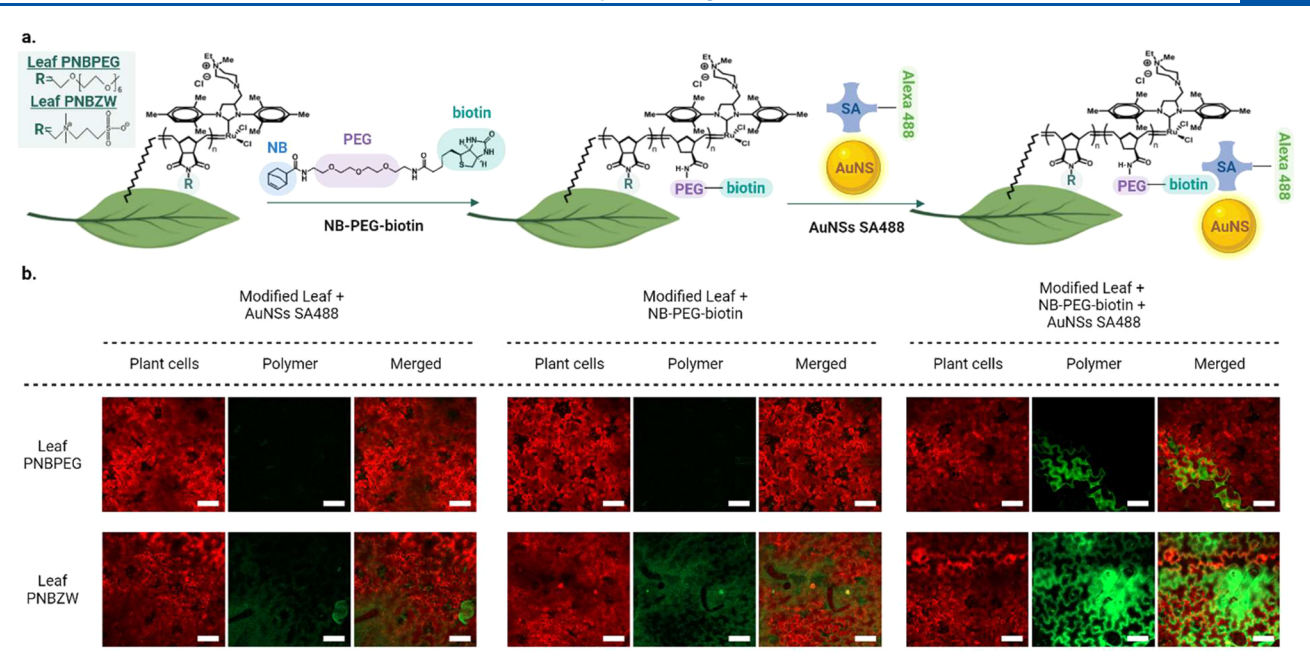


Figure 4. (a) Schematic representation of the attachment of AuNSs SA 488 to the polymeric layers after their modification with NB-PEG-biotin. (b) Confocal microscopy images of modified leaf surfaces with AuNSs SA 488, NB-PEB-biotin, and NB-PEG-biotin + AuNSs SA 488. Red fluorescence is related to the plant cell tissues, while green fluorescence in the last three columns represents the modified polymers with NB-PEG-biotin + AuNSs SA 488. Successful attachment of AuNSs SA 488 demonstrates the modifiability of the biohybrid systems. Scale bars are 100 μm.

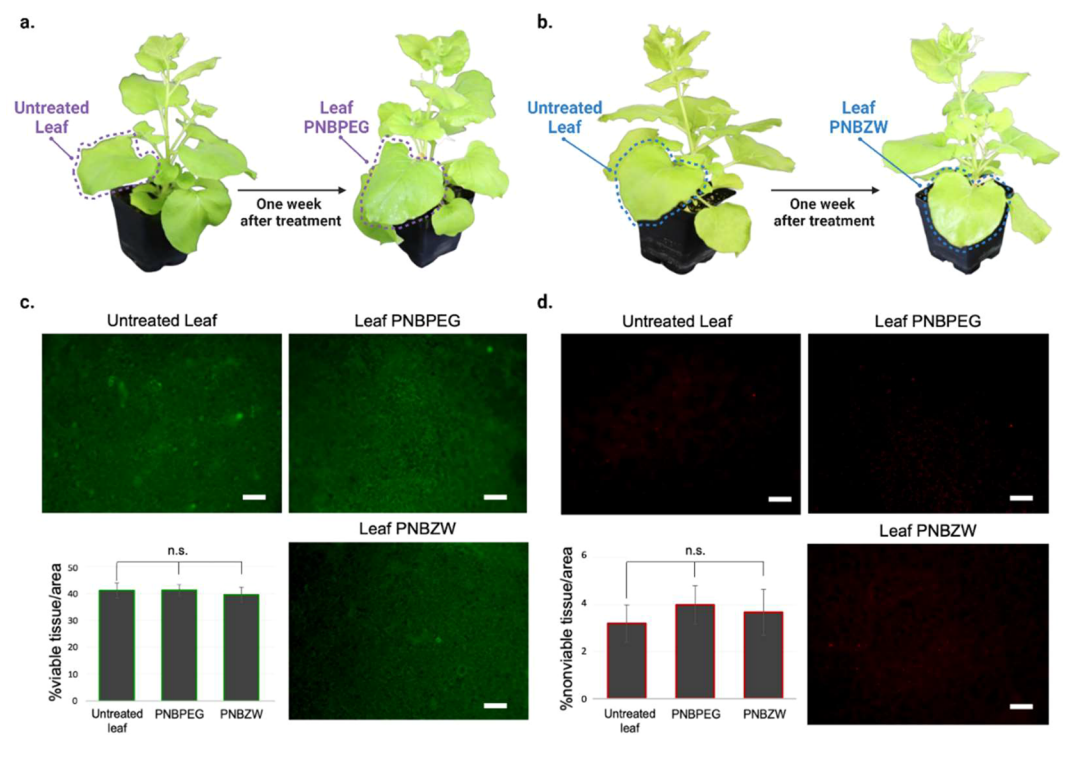


Figure 5. Plants after 1 week of their modification by the incorporation of (a) PNBPEG and (b) PNBZW. Biocompatibility assay using fluorescence microscopy images of modified leaves surfaces. (c) Green fluorescence refers to viable cells stained with fluorescence idiacetate; while (d) red fluorescence refers to nonviable cells stained with propidium iodide (PI; P < 0.05; n = 5).

on the leaf surfaces could prevent stress responses in the plant and potential damage. As elaborated in subsequent sections, our findings indicate that the health of plant—polymer biohybrid systems remains similar to untreated leaves.

The ability to modify the polymeric layer to introduce new functionality was confirmed by introducing an additional block consisting of norbornene polyethylene glycol biotin (NB-PEG- biotin) monomers. Subsequently, these block polymers were modified by attaching gold nanospheres (AuNSs) conjugated to Alexa Fluor 488 streptavidin (AuNSs SA488) (Figure 4a). The selection of AuNSs was based on their ability to enhance the stability and fluorescence signal of the Alexa Fluor 488 streptavidin unit without interfering with the streptavidin—biotin interaction. ^{33,34} The successful confirmation of this

modification was assessed through confocal microscopy, with a focus on the fluorescence of Alexa Fluor 488, as well as quantification of gold using ICP-MS to determine the amount of AuNSs present.

We conducted an examination of the modified leaves using confocal microscopy following their modification with either NB-PEG-biotin or AuNSs SA488. This analysis revealed primarily red fluorescence, which corresponds to the chlorophyll in the plant cell tissues when excited at 638 nm (Figure 4b). In contrast, modified leaves treated successively with NB-PEG-biotin and AuNSs SA488 exhibited green fluorescence, corresponding to the Alexa Fluor 488 upon excitation at 488 nm. These results confirm the formation of the block polymer through the attachment of the AuNSs SA488 to the polymer formed by the NB-PEG-biotin monomers. For a quantitative assessment of the system's modifiability, we analyzed gold concentrations using ICP-MS. An approximate 5-fold increase in concentrations of gold was observed in samples modified with NB-PEG-biotin and AuNSs SA488, compared to the control samples without biotin, further indicating specific binding to the biotinylated monomer (Figure S2).

Plants exhibited no apparent morphological damage within 1 week after undergoing modification (Figure 5a,b). Furthermore, the plant-polynorbornene biohybrid systems viability is comparable to wild-type Nicotiana benthamiana plants after 24 h (Figure 5c,d). We assessed the impact of the polymer in leaves by a cell viability assay using fluorescein diacetate (FD) and propidium iodide (PI). Fluorescence microscopy images of FD-stained leaf mesophyll cells were assessed (Figure 5c). FD is the optimal dye for staining viable plant cells since it is hydrolyzed to highly polar fluorescent compounds that are unable to diffuse across the plasma membrane and are retained within the cytoplasm, producing an intense green fluorescence.³⁵ Image analysis indicated no significant differences in the percentage of viable tissue per leaf area for most treated plants compared with nontreated counterparts. To further assess the biocompatibility of the polymers, leaf disks were also stained with PI to indicate the percentage of dead cells per leaf area (Figure 5d). PI can only enter cells with damaged membranes, where they intercalate into double-stranded nucleic acids.³⁶ Image analysis using ImageJ demonstrated that there was no statistical difference between PNBPEG and PNBZW treated plants and nontreated counterparts. Furthermore, the maximum percentage of nonviable cells/area was ~5%, suggesting high biocompatibility of all the plantpolymer biohybrids, indicating there is not acute toxicity of the polymer coating.

In summary, plant—polynorbornene-derived polymer biohybrid systems were fabricated by the polymerization of NBPEG and NBZW on *Nicotiana benthamiana* leaf surfaces using a biocompatible ROMP strategy. We demonstrated that these systems can be fabricated by the subsequent addition of AM and norbornene-derived monomers via spray coating, which opens opportunities for large-scale plant modification. We envision that the versatility of these systems can lead to the generation of thermal barriers, plant biosensors, nutrient delivery systems, and crop protection layers on plant surfaces, which could serve to increase plant resistance to stressors associated with climate change. Importantly, we verified the methodology developed did not cause acute damage in plant tissues, demonstrating the biocompatibility of the fabrication strategy.

ASSOCIATED CONTENT

Supporting Information

The Supporting Information is available free of charge at https://pubs.acs.org/doi/10.1021/acsmacrolett.4c00297.

Additional experimental details, materials, methods, and images (PDF)

AUTHOR INFORMATION

Corresponding Authors

Jonathan K. Pokorski — Department of NanoEngineering, University of California San Diego, La Jolla, California 92093, United States; Center for Nano-ImmunoEngineering, Institute for Materials Discovery and Design, and Center for Engineering in Cancer, Institute for Engineering in Medicine, University of California San Diego, La Jolla, California 92093, United States; ◎ orcid.org/0000-0001-5869-6942; Email: jpokorski@ucsd.edu

Nicole F. Steinmetz — Department of NanoEngineering, University of California San Diego, La Jolla, California 92093, United States; Department of Bioengineering, Department of Radiology, Center for Nano-ImmunoEngineering, Institute for Materials Discovery and Design, Moores Cancer Center, and Center for Engineering in Cancer, Institute for Engineering in Medicine, University of California San Diego, La Jolla, California 92093, United States; Occid.org/0000-0002-0130-0481;

Email: nsteinmetz@ucsd.edu

Authors

Luis Palomino — Department of NanoEngineering, University of California San Diego, La Jolla, California 92093, United States; Institute for Materials Discovery and Design, University of California San Diego, La Jolla, California 92093, United States

Ivonne Gonzalez-Gamboa — Department of NanoEngineering, University of California San Diego, La Jolla, California 92093, United States; Department of Molecular Biology, Shu and K. C. Chien and Peter Farrell Collaboratory, Center for Nano-ImmunoEngineering, and Institute for Materials Discovery and Design, University of California San Diego, La Jolla, California 92093, United States

Moises Garcia-Mendoza — Department of NanoEngineering, University of California San Diego, La Jolla, California 92093, United States

Andrea G. Monroy-Borrego – Department of NanoEngineering, University of California San Diego, La Jolla, California 92093, United States; Institute for Materials Discovery and Design, University of California San Diego, La Jolla, California 92093, United States

Lisa Tang — Department of NanoEngineering, University of California San Diego, La Jolla, California 92093, United States; Chemical Engineering Program and Institute for Materials Discovery and Design, University of California San Diego, La Jolla, California 92093, United States;

orcid.org/0000-0001-5312-673X

Bin Wang — Department of NanoEngineering, University of California San Diego, La Jolla, California 92093, United States; Institute for Materials Discovery and Design, University of California San Diego, La Jolla, California 92093, United States; orcid.org/0000-0002-9373-5684

Andrea Tao — Department of NanoEngineering, University of California San Diego, La Jolla, California 92093, United States; Institute for Materials Discovery and Design, University of California San Diego, La Jolla, California 92093, United States; orcid.org/0000-0003-1857-8743

Jinhye Bae — Department of NanoEngineering, University of California San Diego, La Jolla, California 92093, United States; Chemical Engineering Program and Institute for Materials Discovery and Design, University of California San Diego, La Jolla, California 92093, United States;

orcid.org/0000-0002-2536-069X

Complete contact information is available at: https://pubs.acs.org/10.1021/acsmacrolett.4c00297

Notes

The authors declare no competing financial interest.

ACKNOWLEDGMENTS

This research was primarily supported by NSF through the UC San Diego Materials Research Science and Engineering Center (UCSD MRSEC) DMR-2011924. The authors acknowledge the use of facilities and instrumentation supported by NSF through the UC San Diego Materials Research Science and Engineering Center (UCSD MRSEC) DMR-2011924. We thank the University of California, San Diego Cancer Center Microscopy core and the NCI P30 Grant 2P30CA023100 for the use of confocal microscopy. Furthermore, authors would like to acknowledge Neal Arakawa of the Environmental and Complex Analysis Laboratory (ECAL) at the University of California San Diego and Ich Tran of the Irvine Materials Research Institute (IMRI) at the University of California Irvine. A.M.B. is supported by CONANCYT for doctoral studies (CVU 1062156). The authors thank Han Sol and Adam Caparco for their support in this project.

REFERENCES

- (1) Introduction to Bioelectronics: Materials, Devices, and Applications; Stavrinidou, E., Proctor, C. M., Eds.; AIP Publishing, 2022. DOI: 10.1063/9780735424470.
- (2) UN focus on plant health, crucial for boosting food security worldwide | UN News. United Nations; https://news.un.org/en/story/2022/05/1118102 (accessed 2023–11–18).
- (3) Ortiz-Bobea, A.; Ault, T. R.; Carrillo, C. M.; Chambers, R. G.; Lobell, D. B. Anthropogenic Climate Change Has Slowed Global Agricultural Productivity Growth. *Nat. Clim. Change* **2021**, *11* (4), 306–312.
- (4) Agnew, J.; Hendery, S. 2023 Global Agricultural Productivity Report: Every Farmer, Every Tool; Virginia Tech College of Agriculture and Life Sciences, 2023.
- (5) Csizmar, C. M.; Petersburg, J. R.; Wagner, C. R. Programming Cell-Cell Interactions through Non-Genetic Membrane Engineering. *Cell Chem. Biol.* **2018**, 25 (8), 931–940.
- (6) Church, D. C.; Pokorski, J. K. Cell Engineering with Functional Poly(Oxanorbornene) Block Copolymers. *Angew. Chem.* **2020**, 132 (28), 11475–11479.
- (7) Church, D. C.; Davis, E.; Caparco, A. A.; Takiguchi, L.; Chung, Y. H.; Steinmetz, N. F.; Pokorski, J. K. Polynorbornene-Based Bioconjugates by Aqueous Grafting-from Ring-Opening Metathesis Polymerization Reduce Protein Immunogenicity. *Cell Rep. Phys. Sci.* **2022**, *3* (10), 101067.
- (8) Chen, W.; Fu, L.; Chen, X. Improving Cell-Based Therapies by Nanomodification. *J. Controlled Release* **2015**, *219*, 560–575.
- (9) Zhou, Z.; Maxeiner, K.; Ng, D. Y. W.; Weil, T. Polymer Chemistry in Living Cells. Acc. Chem. Res. 2022, 55 (20), 2998–3009.

- (10) Davis, E.; Caparco, A. A.; Steinmetz, N. F.; Pokorski, J. K. Poly(Oxanorbornene)-Protein Conjugates Prepared by Grafting-to ROMP as Alternatives for PEG. *Macromol. Biosci.* **2024**, *24*, 2300255.
- (11) Stavrinidou, E.; Gabrielsson, R.; Gomez, E.; Crispin, X.; Nilsson, O.; Simon, D. T.; Berggren, M. Electronic Plants. *Sci. Adv.* **2015**, *1* (10), No. e1501136.
- (12) Stavrinidou, E.; Gabrielsson, R.; Nilsson, K. P. R.; Singh, S. K.; Franco-Gonzalez, J. F.; Volkov, A. V.; Jonsson, M. P.; Grimoldi, A.; Elgland, M.; Zozoulenko, I. V.; Simon, D. T.; Berggren, M. In Vivo Polymerization and Manufacturing of Wires and Supercapacitors in Plants. *Proc. Natl. Acad. Sci. U. S. A.* **2017**, *114* (11), 2807–2812.
- (13) Parker, D.; Daguerre, Y.; Dufil, G.; Mantione, D.; Solano, E.; Cloutet, E.; Hadziioannou, G.; Näsholm, T.; Berggren, M.; Pavlopoulou, E.; Stavrinidou, E. Biohybrid Plants with Electronic Roots *via in Vivo* Polymerization of Conjugated Oligomers. *Mater. Horiz.* **2021**, 8 (12), 3295–3305.
- (14) Zhao, J.; Ma, Y.; Steinmetz, N. F.; Bae, J. Toward Plant Cyborgs: Hydrogels Incorporated onto Plant Tissues Enable Programmable Shape Control. *ACS Macro Lett.* **2022**, *11* (8), 961–966.
- (15) Yu, A. C.; Reinhart, M.; Hunter, R.; Lu, K.; Maikawa, C. L.; Rajakaruna, N.; Acosta, J. D.; Stubler, C.; Appel, C.; Appel, E. A. Seasonal Impact of Phosphate-Based Fire Retardants on Soil Chemistry Following the Prophylactic Treatment of Vegetation. *Environ. Sci. Technol.* **2021**, *55* (4), 2316–2323.
- (16) Dufil, G.; Bernacka-Wojcik, I.; Armada-Moreira, A.; Stavrinidou, E. Plant Bioelectronics and Biohybrids: The Growing Contribution of Organic Electronic and Carbon-Based Materials. *Chem. Rev.* **2022**, 122 (4), 4847–4883.
- (17) Buriak, J. M.; Liz-Marzán, L. M.; Parak, W. J.; Chen, X. Nano and Plants. ACS Nano 2022, 16 (2), 1681–1684.
- (18) Church, D. C.; Takiguchi, L.; Pokorski, J. K. Optimization of Ring-Opening Metathesis Polymerization (ROMP) under Physiologically Relevant Conditions. *Polym. Chem.* **2020**, *11* (27), 4492–4499.
- (19) Isarov, S. A.; Pokorski, J. K. Protein ROMP: Aqueous Graftfrom Ring-Opening Metathesis Polymerization. *ACS Macro Lett.* **2015**, *4* (9), 969–973.
- (20) Isarov, S. A.; Lee, P. W.; Pokorski, J. K. Graft-to" Protein/Polymer Conjugates Using Polynorbornene Block Copolymers. *Biomacromolecules* **2016**, *17* (2), 641–648.
- (21) Lee, P. W.; Isarov, S. A.; Wallat, J. D.; Molugu, S. K.; Shukla, S.; Sun, J. E. P.; Zhang, J.; Zheng, Y.; Lucius Dougherty, M.; Konkolewicz, D.; Stewart, P. L.; Steinmetz, N. F.; Hore, M. J. A.; Pokorski, J. K. Polymer Structure and Conformation Alter the Antigenicity of Virus-like Particle-Polymer Conjugates. *J. Am. Chem. Soc.* 2017, 139 (9), 3312–3315.
- (22) Arya, G. C.; Sarkar, S.; Manasherova, E.; Aharoni, A.; Cohen, H. The Plant Cuticle: An Ancient Guardian Barrier Set Against Long-Standing Rivals. *Front. Plant Sci.* **2021**, *12*, 663165.
- (23) Negin, B.; Hen-Avivi, S.; Almekias-Siegl, E.; Shachar, L.; Jander, G.; Aharoni, A. Tree Tobacco (*Nicotiana Glauca*) Cuticular Wax Composition Is Essential for Leaf Retention during Drought, Facilitating a Speedy Recovery Following Rewatering. *New Phytol.* **2023**, 237 (5), 1574–1589.
- (24) Ohlmann, D. M.; Tschauder, N.; Stockis, J.-P.; Gooßen, K.; Dierker, M.; Gooßen, L. J. Isomerizing Olefin Metathesis as a Strategy To Access Defined Distributions of Unsaturated Compounds from Fatty Acids. *J. Am. Chem. Soc.* **2012**, *134* (33), 13716–13729.
- (25) Nagyházi, M.; Lukács, Á.; Turczel, G.; Hancsók, J.; Valyon, J.; Bényei, A.; Kéki, S.; Tuba, R. Catalytic Decomposition of Long-Chain Olefins to Propylene via Isomerization-Metathesis Using Latent Bicyclic (Alkyl)(Amino)Carbene-Ruthenium Olefin Metathesis Catalysts. *Angew. Chem., Int. Ed.* **2022**, *61* (28), na DOI: 10.1002/anie.202204413.
- (26) Török, B.; Schäfer, C.; Kokel, A. Metathesis by Heterogeneous Catalysts. *Heterogeneous Catalysis in Sustainable Synthesis*; Elsevier, 2022; pp 279–316. DOI: 10.1016/B978-0-12-817825-6.00004-5.
- (27) Nieres, P. D.; Vaillard, V. A.; Zelín, J.; Neuman, N. I.; Trasarti, A. F.; Apesteguía, C. R.; Vaillard, S. E. Stability of a Silica-Supported

- Second Generation Hoveyda-Grubbs Catalyst Under Atmospheric Conditions: Experimental and Computational Studies. *ChemCatChem.* **2023**, *15* (10), No. e202300010.
- (28) Balcerzak, J.; Redzynia, W.; Tyczkowski, J. In-Situ XPS Analysis of Oxidized and Reduced Plasma Deposited Ruthenium-Based Thin Catalytic Films. *Appl. Surf. Sci.* **2017**, *426*, 852–855.
- (29) Benitez-Medina, G. E.; Flores, R.; Vargas, L.; Cuenú, F.; Sharma, P.; Castro, M.; Ramírez, A. Hybrid Material by Anchoring a Ruthenium(II) Imine Complex to SiO 2: Preparation, Characterization and DFT Studies. *RSC Adv.* **2021**, *11* (11), 6221–6233.
- (30) Jarzembska, K.; Seal, S.; Wozniak, K.; Szadkowska, A.; Bieniek, M.; Grela, K. X-ray Photoelectron Spectroscopy and Reactivity Studies of a Series of Ruthenium Catalysts. *ChemCatChem.* **2009**, *1*, 144–151.
- (31) Noffke, A. L.; Habtemariam, A.; Pizarro, A. M.; Sadler, P. J. Designing Organometallic Compounds for Catalysis and Therapy. *Chem. Commun.* **2012**, 48 (43), 5219.
- (32) Al-Enezi, M. Y.; John, E.; Ibrahim, Y. A.; Al-Awadi, N. A. Highly Efficient Ru(11)-Alkylidene Based Hoveyda-Grubbs Catalysts for Ring-Closing Metathesis Reactions. *RSC Adv.* **2021**, *11* (60), 37866–37876.
- (33) Reis, D. S.; De Oliveira, V. L.; Silva, M. L.; Paniago, R. M.; Ladeira, L. O.; Andrade, L. M. Gold Nanoparticles Enhance Fluorescence Signals by Flow Cytometry at Low Antibody Concentrations. J. Mater. Chem. B 2021, 9 (5), 1414–1423.
- (34) Conrad, M.; Proll, G.; Builes-Münden, E.; Dietzel, A.; Wagner, S.; Gauglitz, G. Tools to Compare Antibody Gold Nanoparticle Conjugates for a Small Molecule Immunoassay. *Microchim. Acta* **2023**, 190 (2), 62.
- (35) Jones, K.; Kim, D. W.; Park, J. S.; Khang, C. H. Live-Cell Fluorescence Imaging to Investigate the Dynamics of Plant Cell Death during Infection by the Rice Blast Fungus Magnaporthe Oryzae. *BMC Plant Biol.* **2016**, *16* (1), 69.
- (36) Wu, H.; Nißler, R.; Morris, V.; Herrmann, N.; Hu, P.; Jeon, S.-J.; Kruss, S.; Giraldo, J. P. Monitoring Plant Health with Near-Infrared Fluorescent H $_2$ O $_2$ Nanosensors. *Nano Lett.* **2020**, 20 (4), 2432–2442.